Journal of Advanced Marine Engineering and Technology, Vol. 50, No. 2, pp. 89~99, 2026
J. Advanced Marine Engineering and Technology (JAMET)
https://doi.org/10.5916/jamet.2026.50.2.89

ISSN 2234-7925 (Print)
ISSN 2765-4796 (Online)
Original Paper

Effect of DC electric-fields on the dynamic behavior of methane jet flame

Juwon Park[1,†]

(Received March 15, 2026 ; Revised March 23, 2026 ; Accepted April 13, 2026)

Abstract: The interaction between electric fields and hydrocarbon flames has attracted significant attention due to its potential applications in combustion control, pollutant reduction, and fire safety. In this study, the dynamic behavior of methane jet flames subjected to externally applied DC electric fields was experimentally investigated with particular emphasis on the influence of electric-field orientation. A methane jet flame was generated using a 4.5 mm inner-diameter nozzle at a constant jet velocity of 12 cm/s. A metallic mesh electrode was positioned 5 cm from the nozzle center, and three electrode orientations relative to the jet axis ($-90°$, $-45°$, and $0°$) were considered. DC voltages ranging from -10 kV to $+10$ kV were applied to examine the combined effects of electric-field strength and orientation. Flame dynamics were recorded using video imaging and analyzed through MATLAB-based image processing to extract flame-tip displacement, deflection angle, and temporal flame motion. Four distinct flame regimes were identified: tilted, lifted, oscillating, and fluctuating flames. Negative voltages produced relatively stable flame deflection or lift-off due to ionic-wind-induced electrohydrodynamic flow toward the electrode, whereas positive voltages generated periodic oscillations and irregular fluctuations. Frequency analysis revealed dominant oscillations within the range associated with Kelvin–Helmholtz instability in buoyant jet flames. Non-dimensional analysis using the Strouhal number, modified electrohydrodynamic number, and Froude number demonstrated that flame dynamics are governed by the competition between electrohydrodynamic forcing, jet inertia, and buoyancy. These results highlight the critical role of electric-field orientation in controlling methane flame behavior.

Keywords: Methane jet flame, Electric field, Flame dynamics, Strouhal number, Froude number

1. Introduction

The strengthening of greenhouse gas emission regulations by the International Maritime Organization (IMO) has led to increasing demand for low-carbon and high-efficiency marine fuels **[1][2]**. Consequently, the adoption of LNG-fueled ships, dual-fuel engines, and gas fuel supply systems has been rapidly expanding in the maritime industry **[3][4]**. As methane (CH_4) constitutes the primary component of LNG fuel, understanding the combustion and safety characteristics of methane-based flames has become increasingly important **[5]-[7]**.

In confined shipboard environments such as engine rooms, fuel supply lines, and fuel processing compartments, accidental gas leakage may result in the formation of free jet flames. The behavior of such flames is closely related to fire hazard assessment, ventilation system design, flame propagation prediction, and the development of effective accident response strategies. Therefore, understanding the dynamic characteristics of methane jet flames under realistic operating conditions is essential for improving fire safety in marine applications **[8][9]**.

Meanwhile, modern ships are becoming increasingly electrified due to the widespread adoption of electric propulsion systems, high-voltage power distribution units, power converters, and battery-based energy storage systems (ESS) **[10][11]**. These electrically intensive environments may generate localized electric fields within shipboard compartments. When flames are present in such environments, the electric field can interact with the combustion zone through the motion of charged species, potentially modifying the surrounding flow field and flame structure. Therefore, investigating the electric-field response of methane flames is not only of fundamental combustion interest but also of practical relevance for fire safety assessment in electrified marine systems.

† Corresponding Author (ORCID: https://orcid.org/0000-0002-1944-5574): Ph. D. Candidate, Department of Marine System Engineering, Korea Maritime & Ocean University, 727, Taejong-ro, Yeongdo-gu, Busan 49112, Korea, E-mail: pjw6642@gmail.com, Tel: +51-410-4261

1 Ph. D. Candidate, Interdisciplinary Major of Maritime AI Convergence, Korea Maritime & Ocean University, E-mail: pjw6642@gmail.com, Tel: +82-51-410-4261

When an external electric field is applied to hydrocarbon flames, charged species generated through chemi-ionization—including positive ions, negative ions, and electrons—migrate under the influence of the electric force. Through collisions with neutral molecules, these charged particles transfer momentum to the surrounding gas, producing a bulk flow motion commonly referred to as "ionic wind" **[12][13]**. This electrohydrodynamically induced flow can influence flame structure, stability, extinction characteristics, soot formation, and mixing processes, and is widely recognized as a dominant mechanism governing flame behavior under electric fields. In the sub-breakdown regime, numerous studies **[14]-[17]** have demonstrated that the primary effect of the electric field is the generation of ionic wind resulting from charged particle drift, while direct modifications of chemical reaction rates or radical concentrations remain negligible. Regardless of whether the electric field is aligned parallel **[14]** or perpendicular **[17]** to the flame propagation direction, the intrinsic flame speed remains essentially unchanged, indicating that flame dynamics are primarily governed by flow-field modification through ion–neutral momentum transfer.

Particularly, free jet flames are characterized by an upward development governed by the combined effects of buoyancy and jet momentum. When an external electric field is applied, the electrohydrodynamic body force induced by the drift motion of charged species can significantly modify this buoyancy-dominated structure. In confined environments such as shipboard spaces, the direction of the electric field does not necessarily coincide with the buoyant direction of the flame. Under such conditions, the electrode geometry and orientation—which determine the spatial non-uniformity of the electric field—may directly influence flame behavior, including flame tilting, oscillation, irregular fluctuations, and lift-off.

However, most previous studies have primarily been conducted under configurations where electrodes were arranged in axisymmetric or nearly symmetric geometries. Consequently, existing research has mainly focused on the influence of electric-field strength itself, while systematic investigations on the directional effects of the electric field on methane jet flame dynamics remain limited **[14]-[16][18]**.

Therefore, in this study, a rectangular mesh electrode was positioned on one side of a methane jet flame, and the flame behavior was experimentally investigated by varying both the electrode orientation and the applied DC electric-field strength. The flame height and lateral displacement relative to the nozzle center were quantitatively tracked using frame-by-frame image processing techniques. Through this approach, the present work aims to elucidate how variations in electric-field strength and polarity modify the buoyancy-driven flame structure.

The findings of this study are expected to provide fundamental insights into the influence of electric-field environments on flame behavior, particularly in scenarios relevant to LNG-fueled ships and gas-leak fires in electrically complex environments.

2. Experimental Method

The experimental setup used in this study is illustrated in **Figure 1**. A circular nozzle with an inner diameter of 4.5 mm was installed vertically to generate a methane jet flame. Pure methane was injected through the nozzle at a fixed nozzle exit velocity of $U_0 = 12$ cm/s, and all experiments were conducted under this single flow condition. The selected jet velocity corresponds to a laminar flow regime, which allows the fundamental interaction between electrohydrodynamic (EHD) forcing and buoyancy-driven jet behavior to be isolated without significant interference from turbulent fluctuations. This approach enables a clearer identification of the underlying physical mechanisms governing flame dynamics.

To generate an external electric field, a rectangular metallic mesh (13 × 10 cm, 1 × 1 cm grid size) was positioned at a distance of 5 cm from the nozzle center. DC electric potential was applied using a function generator (Keysight 33500b series) and high voltage amplifier (Trek 10/10B-Hs). To generate an electric field, high voltage was applied to the rectangular metallic mesh

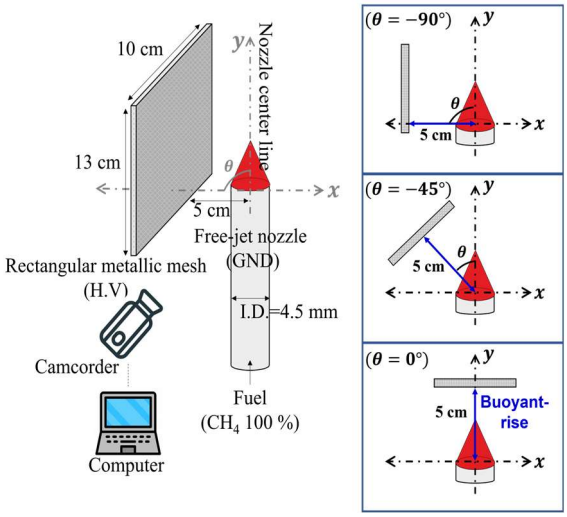

Figure 1: Experimental setup of the methane jet flame under DC electric fields with different angles of mesh

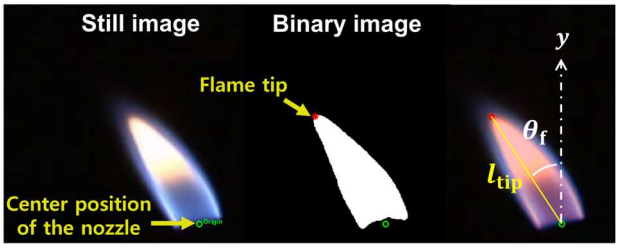

Figure 2: Image-processing procedure for flame tip position and deflection angle

and the fuel nozzle served as a ground (GND). The applied DC voltages ranged from $V_{DC} = -10$ to $+10$ kV with increments of 2 kV and were monitored using 1000:1 high-voltage probe (Tektronix, P6015A) and oscilloscope (Teledyne MDO34). In order to investigate the influence of electric-field orientation on flame behavior, the angular position of the mesh electrode relative to the nozzle center was varied. Specifically, three electrode orientations were considered: a lateral configuration ($\theta = -90°$), an oblique configuration ($\theta = -45°$), and an axial configuration ($\theta = 0°$), where the angle was defined based on the viewing direction from the nozzle center. For all configurations, the distance between the nozzle center and the mesh electrode was maintained at 5 cm. As a result, a total of 30 experimental cases were examined by combining the three electrode orientations with ten voltage conditions.

All flame images were recorded using an optical camcorder (Canon VIXIA HF G50) connected to a PC, capturing video at 60 frames per second (fps) and subsequently analyzed using image-processing techniques implemented in MATLAB. In addition, the recorded video data were used to measure the flame height and to perform Fast Fourier Transform (FFT) analysis. For all experimental conditions, flame images were recorded for more than 10 seconds to ensure sufficient temporal resolution for the analysis. Considering that the number of data points used in FFT analysis must be a power of 2, a sequence of 512 consecutive frames was selected for the frequency analysis. The flame height was extracted from each image using the image-processing procedure described earlier, and the resulting time-series dataset of flame-tip positions was constructed. FFT analysis was then applied to this time-series dataset to identify the dominant oscillation frequencies and to characterize the dynamic flame behavior with high temporal accuracy.

The overall image analysis procedure is illustrated in **Figure 2**. First, the captured flame images were converted into binary images through a binarization process in order to isolate the flame region from the background. During this step, the threshold level was selected to identify the main luminous reaction zone of the jet flame, which corresponds to the stoichiometric reaction layer. The faint outer blue flame envelope observed beyond the main reaction zone was excluded from the flame tip detection to ensure consistent identification of the flame boundary.

After binarization, the nozzle center was defined as the origin of the coordinate system. The flame tip was determined as the outermost point of the detected flame region with respect to the nozzle center. The corresponding x and y pixel coordinates of the flame tip were extracted for each frame, and these pixel coordinates were converted into physical distances using the spatial calibration of the imaging system.

Using the extracted flame tip coordinates, the distance from the nozzle center to the flame tip and the flame deflection angle were calculated. By tracking the temporal evolution of the flame tip position, various flame behaviors such as tilting, lift-off, periodic oscillation, and irregular fluctuations were quantitatively characterized under different electric-field conditions.

3. Results and Discussion

3.1 Overall flame behavior under applied V_{DC}

Figure 3 shows the baseline flame images obtained without the application of an electric field for the three electrode orientations. The baseline flames formed under these conditions exhibited similar flame heights of approximately 2.1–2.2 cm, indicating that the electrode position itself does not significantly influence the flame structure in the absence of an electric field.

The overall flame behaviors observed under different electrode orientations and applied DC voltages are summarized in **Table 1**. The methane jet flames subjected to the electric field exhibited five distinct dynamic regimes: stable flame, tilted flame, lifted flame, oscillating flame, and fluctuating flame. These regimes were identified based on the temporal evolution of the flame tip position and the visual flame structure extracted from the image analysis.

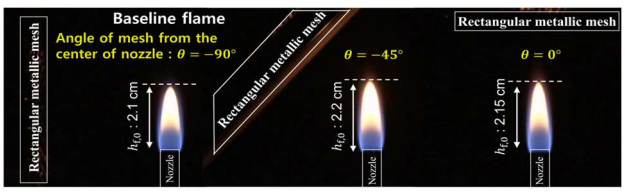

Figure 3: Baseline flames without electric fields for different angles of the electrode

Table 1: Overall flame behavior

Pol.	Applied voltage, V_{DC} [kV]	$\theta = -90°$	$\theta = -45°$	$\theta = -0°$
−	2	Tilted	Tilted	Stable
	4–10			Lifted
+	2	Tilted	Oscillating	Oscillating
	4			Fluctuating
	6		Fluctuating	
	8–10	Fluctuating		

When a negative voltage was applied to the mesh electrode, the flame behavior strongly depended on the orientation of the electric field relative to the jet flow direction. In the lateral and oblique configurations, the flame was consistently deflected toward the electrode, forming a stable tilted flame structure. This behavior can be attributed to electrohydrodynamic (EHD) flow induced by the bulk motion of charged species generated in the reaction zone of hydrocarbon flames through chemi-ionization processes.

Under an applied electric field, charged particles produced by chemi-ionization are accelerated by the Lorentz force. The accelerated ions transfer momentum to surrounding neutral molecules through collisions, generating a bulk gas motion commonly referred to as ionic wind. This ionic wind modifies the local flow structure surrounding the flame.

In hydrocarbon flames, the dominant charged species responsible for the ionic wind effect are positive ions generated within the reaction zone where representative ions include CHO^+ and H_3O^+. Although electrons possess significantly higher mobility than positive ions, their extremely small mass results in a relatively small contribution to momentum transfer. Consequently, the net momentum transfer to the neutral flow is primarily governed by the motion of positive ions drifting toward the cathode.

In addition to ionic wind, the distribution of space charge plays a crucial role in determining the polarity-dependent flame behavior under DC electric fields. Owing to the substantial difference in mobility between electrons and heavy positive ions, a non-uniform charge distribution is established within the flame. Electrons are rapidly transported toward the anode, whereas positive ions tend to accumulate in the reaction zone, resulting in the formation of a space-charge region. This charge separation modifies the local electric field and enhances the EHD body force. Under negative voltage conditions, the drift of positive ions toward the electrode generates a relatively stable ionic wind aligned with the electric field direction, leading to steady flame deflection or lift-off depending on the electrode orientation. In contrast, under positive voltage conditions, the redistribution of space charge near the grounded nozzle intensifies the local electric field gradient and promotes the formation of a shear layer opposing the jet flow. This enhanced shear interaction, combined with the non-uniform EHD body force, destabilizes the flow field and facilitates the transition from stable flame structures to oscillatory and fluctuating regimes.

As a result, under positive voltage conditions, the flame behavior exhibits increasingly complex dynamics with increasing electric field strength. At relatively low positive voltages ($2-6$ kV), the flame maintains a tilted structure toward the electrode. However, when the applied voltage exceeded approximately 8 kV, strong electrohydrodynamic forcing disrupts the laminar jet structure, leading to irregular flame-tip motion accompanied by soot formation. This behavior is characterized as a fluctuating flame regime with non-periodic oscillations.

The oblique configuration exhibited an intermediate behavior between the lateral and axial cases. At relatively low positive voltages ($2-4$ kV), periodic oscillations of the flame tip were observed. This oscillatory motion corresponds to oscillating flames characterized by periodic variations in both flame height and deflection angle. As the applied voltage increased beyond 6 kV, the periodic oscillations gradually transitioned into irregular fluctuations similar to those observed in the lateral configuration. This transition suggests that the increasing electric force destabilizes the balance between jet inertia, buoyancy-induced flow, and electrohydrodynamic forcing.

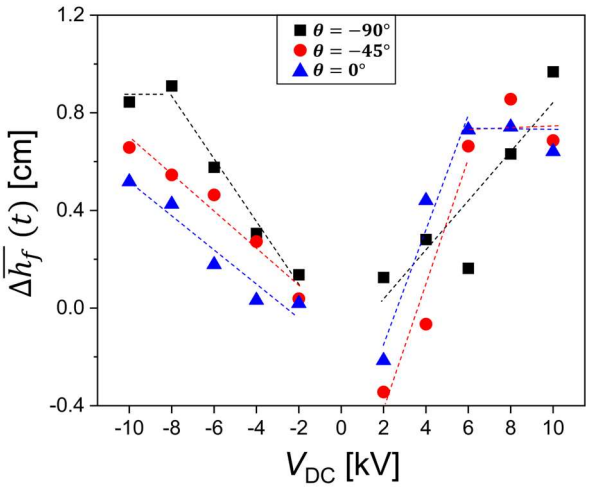

Figure 4: Variation of flame tip height under applied V_{DC}

A similar trend was observed in the axial configuration, where oscillatory behavior appeared at relatively low positive voltages. In this configuration, the electric force acts opposite to the jet flow direction. The interaction between the upward jet inertia and the downward electrohydrodynamic forcing generates a shear layer near the flame base. This shear layer promotes hydrodynamic instability and induces periodic oscillations of the flame tip. As the applied voltage further increases, the interaction becomes increasingly unstable, leading to irregular fluctuations accompanied by strong flame contraction toward the nozzle.

Figure 4 shows the variation of flame tip height under different applied DC voltages. The values plotted on the y-axis represent the time-averaged difference between the flame tip height under electric-field conditions and the baseline flame height. The averaging was performed over a 5 s interval to account for temporal variations in flame tip observed in oscillating and fluctuating flame regimes.

A clear polarity dependent behavior can be observed in **Figure 4**. Under negative voltage conditions, the difference of flame height increases monotonically with increasing electric-field strength, and the magnitude of this increase strongly depends on the electrode orientation. This trend indicates that the electrohydrodynamic forcing generated by ionic wind enhances the overall displacement of the flame away from the nozzle.

As discussed previously, ionic wind is primarily generated by the bulk motion of positive ions formed within the reaction zone. In the lateral and oblique electrode configurations, the EHD forcing acts primarily in the lateral direction relative to the jet axis. Consequently, the flame is deflected toward the electrode while maintaining a relatively stable structure. Because the flame tip follows an oblique trajectory rather than a purely vertical path, the projected axial flame-height difference increases as the electric-field strength increases. This behavior explains the gradual increase in the averaged flame-height difference observed under negative voltage conditions. Furthermore, configurations with stronger lateral electric-field components exhibit larger height variations, indicating stronger flame deflection induced by ionic wind.

In contrast, the axial configuration exhibits a different response. In this case, the electric field is aligned with the jet flow direction, and the electrohydrodynamic force therefore acts along the same axis as the incoming methane jet. When negative voltage is applied, the resulting ionic wind enhances the axial momentum of the flow, effectively increasing the upward convective transport within the reaction zone. As a result, the flame base detaches from the nozzle and a lifted flame structure is formed.

A different trend appears under positive voltage conditions. In the lateral configuration, the flame still exhibits a tilted structure at relatively low voltages ($2-6$ kV), producing flame-height differences comparable to those observed under negative voltage conditions. However, when the applied voltage exceeds approximately 8 kV, the flame dynamics become significantly unstable. The flame tip begins to exhibit irregular motion associated with fluctuations. These fluctuations intermittently cause the flame to contract toward the nozzle, resulting in a substantial decrease in the time-averaged flame height.

In the oblique and axial configurations, these instabilities appear at much lower positive voltages. In these configurations, the electric field contains a strong axial component that directly interacts with the upward jet flow. When a positive voltage is applied to the mesh electrode, the bulk motion of positive ions is reversed compared with the negative voltage condition. The resulting ionic wind partially opposes the upward jet flow, generating a shear layer near the flame base. This shear interaction destabilizes the flame structure and promotes hydrodynamic instabilities, which manifest as oscillatory or fluctuating flame motion.

At relatively low positive voltages in the oblique and axial configurations, periodic oscillatory motion of the flame is observed. In this regime, the flame repeatedly stretches and contracts, producing periodic temporal variations in the flame tip. During the stretching phase, the flame tip often extends above the baseline flame height. Consequently, the time-averaged height difference can become negative in some cases. As the electric-field strength increases further, the oscillatory motion transitions into irregular fluctuations characterized by rapid flame contraction toward the nozzle. This behavior explains the sharp decrease in the averaged flame height observed under high positive voltage conditions.

To further investigate the influence of electrode orientation on flame behavior, the variation of the flame tip deflection angle under negative voltage conditions was analyzed, as shown in **Figure 5**. The x-axis represents the applied negative voltage, while the y-axis shows the time-averaged flame-tip deflection angle over a 5 s. This analysis was restricted to negative voltage cases because the flame behavior under positive voltage conditions was dominated by oscillatory and fluctuating motions. These highly unstable regimes produce large temporal variations

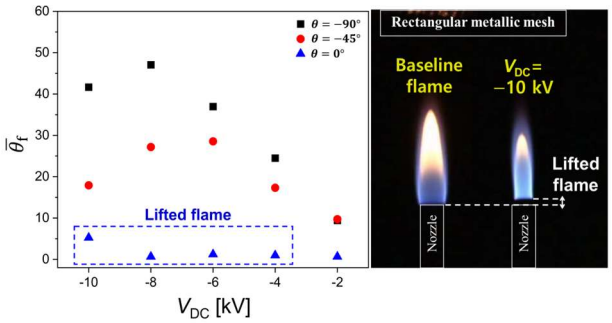

Figure 5: Effect of electrode orientation on flame deflection under negative voltage conditions

in flame-tip position, making it difficult to extract representative deflection angles for comparison between different electrode orientations.

In the axial electrode configuration, the flame exhibited a lifted structure rather than lateral deflection. At -8 kV, the electric field was relatively weak, and the flame remained nearly identical to the baseline flame, indicating that the electrohydrodynamic forcing was insufficient to significantly alter the jet structure. As the magnitude of the negative voltage increased, the flame gradually lifted from the nozzle exit.

This lifted flame behavior occurs because the electric field is aligned with the jet flow direction. Under negative voltage conditions, positive ions generated in the reaction zone are accelerated toward the mesh electrode, producing an axial ionic wind in the same direction as the methane jet. The resulting electrohydrodynamic flow enhances upward convective transport within the flame region, effectively increasing the axial velocity within the reaction zone.

At the highest negative voltage condition (-10 kV), a slight variation in the flame-tip angle was observed even in the axial configuration. This phenomenon can be attributed to instability in the lifted flame base. As the flame lifts further from the nozzle, the anchoring region near the nozzle exit weakens, and the reaction layer near the flame base becomes intermittently disturbed by the incoming jet flow. These disturbances generate small lateral perturbations within the reaction zone, leading to minor variations in the measured deflection angle.

In the oblique configuration, the flame exhibited a clearly tilted structure toward the mesh electrode. Unlike the axial configuration, the electric field in this case possesses both axial and lateral components relative to the jet flow direction. Consequently, the electrohydrodynamic forcing induces a combined flow effect consisting of upward acceleration and lateral deflection. As the magnitude of the negative voltage increases, the lateral ionic wind becomes stronger, and the flame deflection angle correspondingly increases. This behavior indicates that the momentum transfer induced by the electric field becomes increasingly dominant compared with the buoyancy-driven flow in determining the flame trajectory.

The lateral configuration exhibited the largest deflection angles among the three electrode orientations. In this configuration, the electric field is fully aligned in the lateral direction relative to the jet axis. As a result, the ionic wind generates a strong cross-flow component around the flame. As the applied negative voltage increases, the lateral momentum transfer induced by electrohydrodynamic forcing becomes increasingly dominant, bending the flame further toward the electrode.

Interestingly, in both the oblique and lateral configurations, the deflection angle did not increase monotonically at the highest negative voltage condition. Instead, a slight decrease in the average deflection angle was observed at -10 kV. This behavior suggests that excessively strong electric field may introduce additional flow disturbances within the reaction zone. One possible explanation is that the intensified generation and transport of charged species under strong electric fields modify the local ionic-wind structure. Previous study has shown that chemi-ionization in hydrocarbon flames produces both positive and negative ions, whose migration under an applied electric field induces bidirectional ionic wind and alters the surrounding flow field. Under sufficiently strong electric fields, the redistribution of space charges and the resulting modification of ionic-wind induced flow may lead to complex interactions with the surrounding air flow, partially counteracting the primary ionic-wind driven deflection **[19]**.

3.2 Positive Polarity Effect on Flame Behavior

This section focuses on the flame behavior observed under positive voltage conditions. **Figure 6** illustrates the temporal evolution of the flame tip together with the corresponding frequency spectra. The upper row of **Figure 6** presents the temporal flame tip height for the three electrode orientations at an applied $V_{DC} = 2$ kV, while the lower row shows the corresponding frequency spectra obtained from Fast Fourier Transform (FFT) analysis.

For the lateral configuration, the flame tip remains nearly stationary throughout the observation period. The temporal variation of the flame tip height is minimal, and the corresponding frequency spectrum does not exhibit any significant peak. This

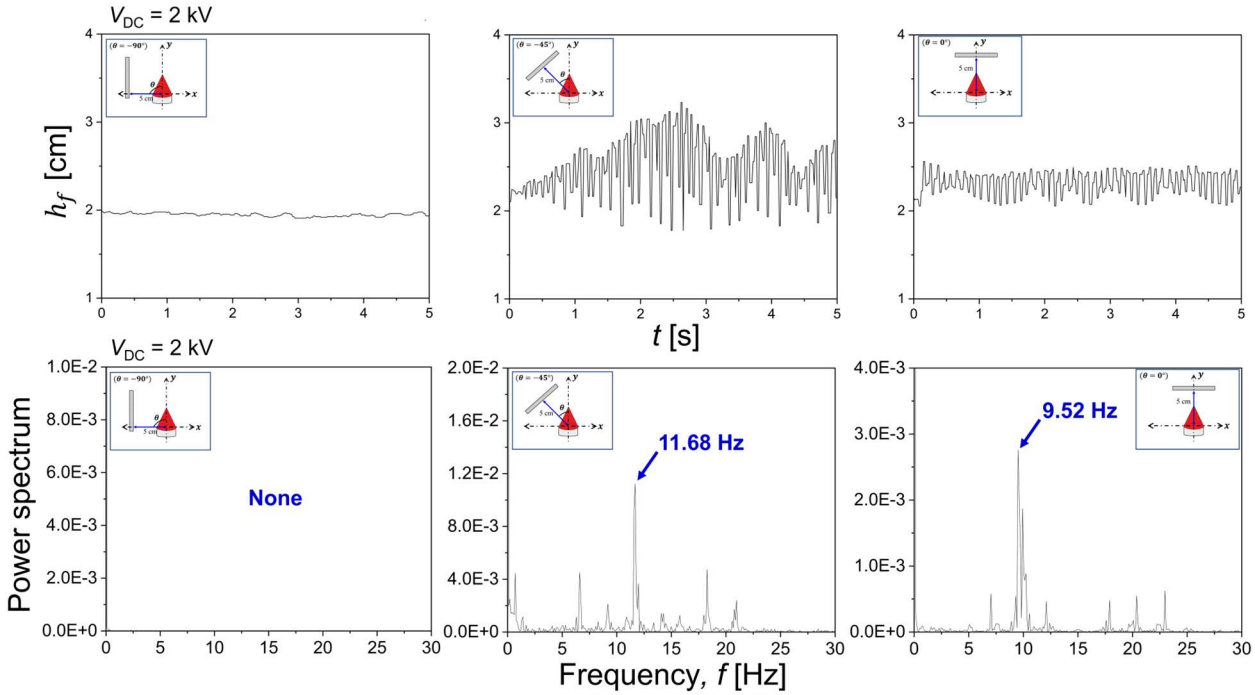

Figure 6: Temporal evolution frequency analysis of oscillating flames at $V_{DC} = 2$ kV

behavior confirms that the flame remains in a stable tilted regime under these conditions. In contrast, the oblique and axial configurations exhibit clear periodic oscillations of the flame tip. The temporal flame tip signals show oscillations in flame height, indicating the presence of periodic flame motion. The corresponding frequency reveals dominant peaks at 11.68 Hz for the oblique configuration and 9.52 Hz for the axial configuration. These peaks correspond to the first harmonic frequency associated with the oscillatory flame motion.

The observed oscillation frequencies fall within the typical frequency range reported for buoyancy-driven instabilities in laminar diffusion flames. Previous studies have shown that Kelvin–Helmholtz (KH) instability can develop in shear layers formed between the jet flow and the surrounding ambient air, leading to periodic oscillations of the flame structure **[20][21]**. In the present experiments, the interaction between the upward jet flow and the electric-field induced ionic wind generates an additional shear layer near the flame base. This shear interaction can amplify hydrodynamic instabilities and promote periodic flame oscillations.

The occurrence of oscillatory motion only in the oblique and axial configurations suggests that the axial component of the electric field plays a critical role in triggering the instability. In these configurations, the electric force interacts directly with the vertical jet momentum, leading to enhanced shear between the upward jet flow and the opposing electrohydrodynamic forcing. This interaction provides a favorable condition for the development of KH instability, which manifests as periodic flame tip oscillations.

To further investigate the oscillatory flame behavior observed under positive voltage conditions, additional experiments were conducted by varying the jet velocity in the electrode configuration of the oblique, where the oscillation phenomenon was most clearly observed. The additional jet velocities considered in this study were 9, 10, and 11 cm/s.

For the applied voltage condition, oscillatory behavior in the additional experiments was observed only at a positive voltage of 3 kV. Therefore, an additional experiment at the baseline jet velocity condition of 12 cm/s was also performed at the same voltage level of 3 kV in order to consistently analyze the oscillation characteristics across different jet velocities.

The oscillatory behavior of the flame was characterized using non-dimensional parameters, as shown in **Figure 7**. The x-axis represents a combined non-dimensional parameter derived from the modified electrohydrodynamic (EHD) number (ψ) and the Froude number (Fr), while the y-axis corresponds to the Strouhal number (St).

The Strouhal number is defined as

$$St = \frac{fD}{U_0} \tag{1}$$

where f is the oscillation frequency, D is the nozzle diameter,

and U_0 is the jet velocity. The Strouhal number represents the ratio between the characteristic oscillation time scale and the convective time scale of the jet flow.

The modified electrohydrodynamic number (ψ) defined as

$$\psi = \sqrt{\frac{\epsilon_0 E_{\text{ext}}^2}{\rho U_0^2}} \tag{2}$$

where ϵ_0 denotes the permittivity of free space (8.85×10^{-12} F/m), E_{ext} is corresponding electric field intensities, defined as V_{DC} divided by the distance from the center of the nozzle to metallic mesh (5 cm), and ρ is the fuel density.

ψ represents the relative magnitude of electrohydrodynamic forcing compared with the inertial force of the flow. Physically, it quantifies the ratio between the electric-field-induced body force and the dynamic pressure of the jet flow **[13]**. A larger value of ψ indicates that electrohydrodynamic forcing plays a more dominant role in determining flame dynamics. The Froude number represents the ratio of inertial force to buoyancy force in the flow and is defined as

$$Fr = \frac{U_0}{\sqrt{gD}} \tag{3}$$

where g is the gravitational acceleration. In buoyant diffusion flames, the Froude number determines the relative importance of jet inertia compared with buoyancy-induced flow.

As shown in **Figure 7**, the oscillatory flame behavior exhibits a clear linear trend when represented using these non-dimensional parameters. The relationship between the parameters can be expressed by the following linear correlation,

$$St = 0.35\frac{1}{\psi Fr^2} - 0.1 \ (R = 0.98) \tag{4}$$

where R denotes the correlation coefficient.

This result suggests that the oscillation frequency is governed by the combined effects of electrohydrodynamic forcing, jet inertia, and buoyancy-induced flow. In particular, the observed linear scaling indicates that the periodic flame motion originates from the interaction between ionic-wind-induced flow and the shear layer formed within the jet flow.

The fluctuating flame regime was analyzed by examining the temporal variation of the flame tip under high positive voltage conditions, as shown in **Figure 8**. In this graph, the time resolved flame tip are presented for the three electrode orientations when

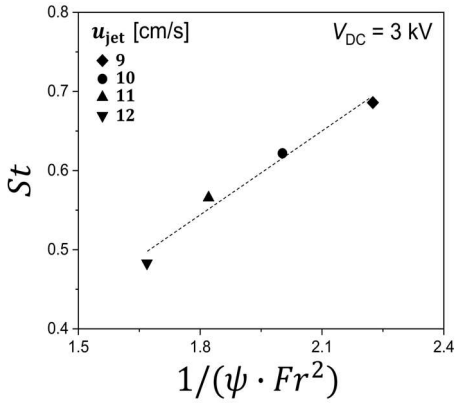

Figure 7: Non-dimensional characterization of oscillating flame behavior

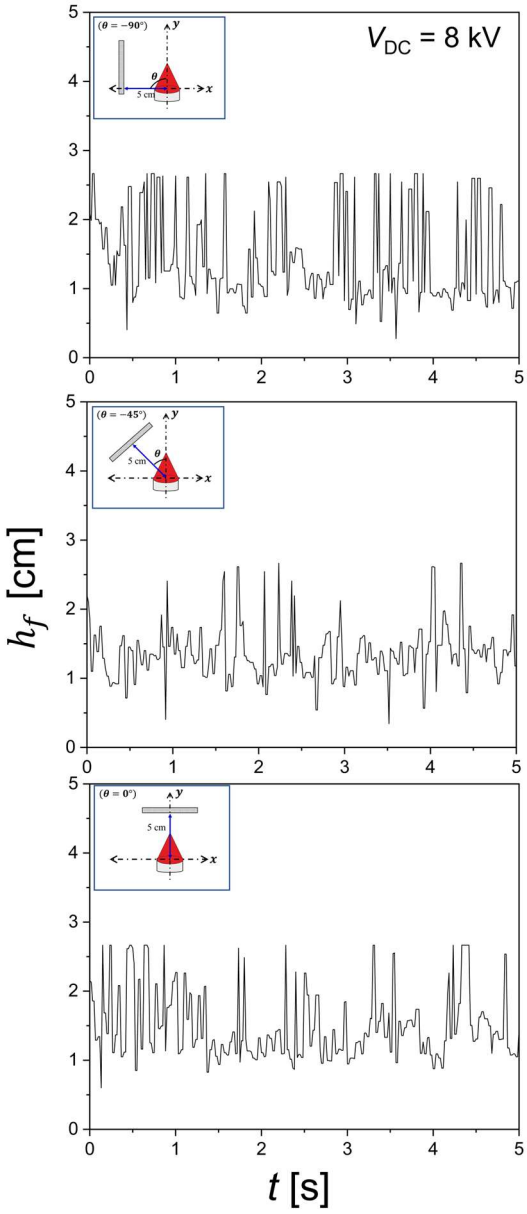

Figure 8: Temporal flame tip fluctuations at $V_{\text{DC}} = 8\ kV$

a voltage of 8 kV was applied. Unlike the oscillatory flame regime, the flame tip motion in this regime does not exhibit a periodic pattern. Instead, the flame tip fluctuates irregularly over time, indicating the presence of non-periodic perturbations in the flame structure.

The transition from oscillatory to fluctuating behavior can be attributed to the increasing dominance of electrohydrodynamic forcing at higher electric-field strengths. As the electric field becomes stronger, the ionic wind induces stronger perturbations in the surrounding flow field. These perturbations can disrupt the laminar structure of the jet flow and generate a large scale vortex near the nozzle.

Furthermore, strong electric fields can enhance ion production near the electrode and modify the local electric-field distribution. These effects can produce complex interactions between the ionic wind, jet flow, and ambient air entrainment. The resulting flow field becomes highly unsteady, leading to irregular flame motions characterized as fluctuating flames.

3.3 Polarity-dependent flame structure and global EHD scaling

Finally, this section discusses the overall characterization of the experimental conditions and the significant differences observed between negative and positive voltage conditions. **Figure 9** presents representative flame images obtained at applied voltages of $+10$ kV and -10 kV for all electrode orientations. Unlike the typical soot-forming structure observed in conventional jet diffusion flames, the jet flames formed under negative voltage conditions exhibit a predominantly blue appearance resembling that of premixed flames.

This behavior can be interpreted in terms of ionic-wind induced mixing enhancement. In hydrocarbon flames, positive ions generated through chemi-ionization within the reaction zone are accelerated toward the negatively charged electrode under negative voltage conditions. The resulting ionic wind transports reactive species and enhances mixing between the fuel jet and ambient oxygen. This enhanced mixing promotes more complete combustion and suppresses soot formation, leading to a predominantly blue flame structure similar to that observed in premixed flames.

In contrast, when a positive voltage is applied to the electrode, the positive ions are accelerated toward the grounded nozzle. The resulting ionic wind partially opposes the upward jet flow and modifies the mixing processes in the reaction zone. In addition, the redistribution of charged species can alter the local flame

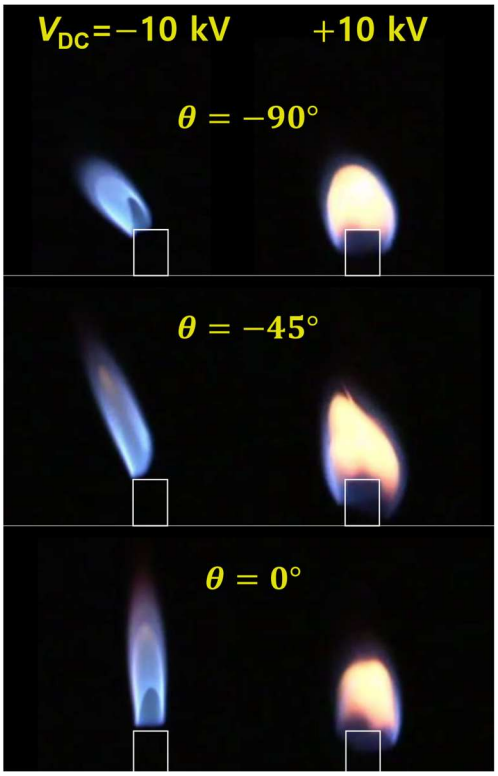

Figure 9: Effect of voltage polarity on flame structure and soot formation

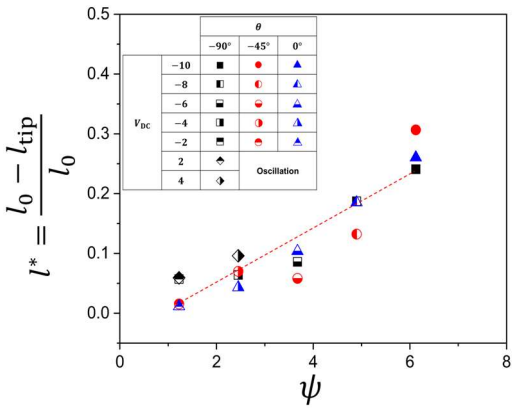

Figure 10: Characterization of flame tip displacement under electric fields

temperature and the residence time of soot precursors. These effects collectively promote soot formation, resulting in bright yellow luminous regions within the flame.

Figure 10 presents a global characterization of the observed flame behavior using non-dimensional parameters. In this graph, the x-axis represents ψ, while the y-axis corresponds to the normalized flame-tip displacement defined as

$$l^* = \frac{l_0 - l_{\text{tip}}}{l_0} \tag{5}$$

where l_{tip} denotes the distance between the center of nozzle and the flame tip when the electric field is applied, and l_0 represents the corresponding distance in the baseline flame without an electric field, which is equivalent to the baseline flame height $h_{\mathrm{f},0}$.

Unlike conventional flame tip height measurements that consider only the vertical displacement of the flame, the present analysis employs the direct distance between the nozzle center and the flame tip. This definition accounts for both vertical displacement and lateral deflection of the flame, which is particularly important in the present experiments where the applied electric field induces significant flame tilting.

The data presented in **Figure 10** exhibit a clear linear trend, indicating that the normalized flame-tip displacement scales well with the electrohydrodynamic forcing parameter. This result suggests that the overall flame behavior is primarily governed by the relative magnitude of the electric-field induced body force compared with the characteristic inertial force of the jet flow.

Oscillating and fluctuating flame cases were excluded from this characterization analysis because the temporal variation of the flame-tip position in these regimes is significantly larger than that in quasi-steady flame regimes. Including these highly unstable cases would obscure the intrinsic scaling relationship associated with quasi-steady flame behaviors such as tilted or lifted flames.

Overall, the results demonstrate that the dynamic behavior of methane jet flames under electric fields can be effectively interpreted in terms of the competition between electrohydrodynamic forcing, jet inertia, and buoyancy-induced flow. The orientation and magnitude of the applied electric field determine the relative contributions of these forces, which ultimately govern the observed flame regimes.

4. Conclusion

This study experimentally investigated the dynamic behavior of methane jet flames subjected to externally applied DC electric fields with varying electrode orientations. By systematically varying both the electrode angle and the applied voltage, the interaction between electrohydrodynamic forcing and buoyancy-driven jet flow was examined. Based on the experimental observations and quantitative image analysis, the main findings of this study can be summarized as follows:

- The methane jet flames exhibited four characteristic behaviors: tilted flames, lifted flames, oscillating flames, and fluctuating flames. These regimes resulted from the interaction between the ionic-wind-induced electrohydrodynamic flow and the intrinsic buoyancy-driven jet flow. In particular, negative voltages primarily produced stable tilted or lifted flames, whereas positive voltages tended to induce oscillatory or fluctuating flame dynamics.
- When the electric field was oriented laterally relative to the jet flow ($\theta = -90°$), the ionic wind generated strong cross-flow momentum, resulting in pronounced flame deflection toward the electrode. In contrast, when the electric field was aligned with the jet axis ($\theta = 0°$), the electrohydrodynamic forcing enhanced axial flow acceleration, leading to lifted flame structures. The oblique configuration ($\theta = -45°$) exhibited intermediate behavior due to the combined influence of axial and lateral electric-force components.
- Periodic oscillations were observed under moderate positive voltage conditions, particularly for electrode orientations containing a significant axial electric-field component. Frequency analysis revealed dominant oscillation frequencies within the typical range of Kelvin–Helmholtz instability observed in buoyant jet flames. The oscillation characteristics were successfully described using non-dimensional parameters including the Strouhal number, modified electrohydrodynamic number, and Froude number, indicating that the oscillation mechanism is governed by the competition between electrohydrodynamic forcing, jet inertia, and buoyancy.
- A non-dimensional characterization based on the modified electrohydrodynamic parameter showed a linear relationship with the normalized flame-tip displacement for quasi-steady flame regimes. This result indicates that the flame behavior can be interpreted through the relative magnitude of the electric-field-induced body force compared with the characteristic inertial forces of the jet flow. The present findings highlight the importance of electric-field orientation in controlling flame dynamics and provide new insights into electrohydrodynamically influenced combustion relevant to electrified energy systems and fire safety applications.

Acknowledgement

This work was supported by Basic Science Research Program through the National Research Foundation of Korea (NRF) funded by the Ministry of Education (No.2021R1I1A3061305).

Author Contributions

Conceptualization, J. Park; Methodology, J. Park; Software, J. Park; Validation, J. Park; Formal Analysis, J. Park; Investigation, J. Park; Resources, J. Park; Data Curation, J. Park; Writing—Original Draft Preparation, J. Park; Writing—Review & Editing, J. Park; Visualization, J. Park; Project Administration, J. Park.

References

[1] International Maritime Organization, 2023 IMO Strategy on Reduction of GHG Emissions from Ships, Resolution MEPC.377(80), 2023.

[2] International Maritime Organization, Fourth IMO Greenhouse Gas Study 2020, London, UK: IMO, 2020.

[3] S. Kumar, H.-T. Kwon, K.-H. Choi, W. Lim, J. H. Cho, K. Tak, and I. Moon, "LNG: An eco-friendly cryogenic fuel for sustainable development," Applied Energy, vol. 88, pp. 4264–4273, 2011.

[4] A. De Carvalho, "Natural gas and other alternative fuels for transportation purposes," Energy, vol. 10, pp. 187–215, 1985.

[5] C. O. Iyogun and M. Birouk, "On the stability of a turbulent non-premixed methane flame," Combustion Science and Technology, vol. 181, pp. 1443–1463, 2009.

[6] O. Yasuhiro and K. Hideaki, "Laminar burning velocity of stoichiometric CH4/air premixed flames at high-pressure and high-temperature," JSME International Journal, vol. 48, pp. 603–609, 2005.

[7] Z. Wang, S. C. Yelishala, G. Yu, H. Metahalchi, and Y. A. Levendis, "Effects of carbon dioxide on laminar burning speed and flame instability of methane/air and propane/air mixtures: A literature review," Energy & Fuels, vol. 33, pp. 9403–9418, 2019.

[8] L. Vandebroek and J. Berghmans, "Safety aspects of the use of LNG for marine propulsion," Procedia Engineering, vol. 45, pp. 21–26, 2012.

[9] N. Bariha, V. C. Srivastava, and I. M. Mishra, "Theoretical and experimental studies on hazard analysis of LPG/LNG release: a review," Reviews in Chemical Engineering, vol. 33, pp. 387–432, 2017.

[10] C. Yao, M. Chen, and Y.-Y. Hong, "Novel adaptive multi-clustering algorithm-based optimal ESS sizing in ship power system considering uncertainty," IEEE transactions on power systems, vol. 33, pp. 307–316, 2018.

[11] J. P. Trovão, F. Machado, and P. G. Pereirinha, "Hybrid electric excursion ships power supply system based on a multiple energy storage system," IET Electrical Systems in Transportation, vol. 6, pp. 145–235, 2016.

[12] M. S. Cha, "Recent understanding with flames under external electric field," 12th Asia-Pacific Conference on Combustion, Fukuoka, Japan, 2019.

[13] J. Lawton, and F. J. Weinberg, Electrical Aspects of Combustion, Clarendon Press, Oxford, U.K., 1969.

[14] S. H. Yoon, B. Seo, J. Park, S. H. Chung, and M. S. Cha, "Edge flame propagation via parallel electric fields in non-premixed coflow jets," Proceedings of the Combustion Institute, vol. 37, pp. 5537–5544, 2019.

[15] D. G. Park, S. H. Chung, and M. S. Cha, "Bidirectional ionic wind in nonpremixed counterflow flames with DC electric fields," Combustion and Flame, vol. 168, pp. 138–146, 2016.

[16] D. G. Park, S. H. Chung, and M. S. Cha, "Visualization of ionic wind in laminar jet flames," Combustion and Flame, vol. 184, pp.246–248, 2017.

[17] M.-V. Tran and M. S. Cha, "Propagating nonpremixed edge-flames in a counterflow, annular slot burner under DC electric fields," Combustion and Flame, vol. 173, pp. 114-122, 2016.

[18] G. T. Kim, D. G. Park, M. S. Cha, J. Park, and S. H. Chung, "Flow instability in laminar jet flames driven by alternating current electric fields," Proceedings of the Combustion Institute, vol. 36, pp.4175–4182, 2017.

[19] Y. Kim, J. Park, D. G. Park, S. H. Yoon, J. Park, and S. H. Chung, "Dynamic behavior of nonpremixed coflow flames with radially applied DC electric fields," Proceedings of the Combustion Institute, vol. 41, p. 105971, 2025.

[20] L. D. Chen, J. P. Seaba, W. M. Roquemore, and L. P. Goss, "Buoyant diffusion flames," Symposium (International) on Combustion, vol. 22, pp.677–684, 1989.

[21] H. Sato, K. Amagai, and M. Arai, "Diffusion flames and their flickering motions related with Froude numbers under various gravity levels," Combustion and Flame, vol. 123 pp. 107–118, 2000.